# WOWA image filters

L. Torres, J. C. Becceneri, C. C. Freitas, S. J. S. Sant'Anna, and S. Sandri

Instituto Nacional de Pesquisas Espaciais (LAC/INPE),
12227-010 - São José dos Campos, SP, Brasil

**Abstract.** We introduce a parametrized family of filters, called WOWA filters, which are based on the WOWA family of mean operators from the fuzzy sets literature. These operators make use of two vectors to weight an input data vector: one whose weights correspond to the same positions in the input, and another that considers the ordered positions of the input. The focus here is on the use of WOWA filters to reduce speckle in SAR imagery. We also address learning the weight vectors with Genetic Algorithms, and compare the proposed filtering approach to a set of filters from the literature, considering SAR images obtained with a single polarization, and $3 \times 3$ windows.

## 1 Introduction

Synthetic Aperture Radar (SAR) sensors can be used at any time of day or night, unlike their optical counterparts. Moreover, they are also not so adversely as optical sensors to atmospheric conditions and the presence of clouds [12]. However, the visual quality of SAR images are degraded by sudden variations in image intensity with a salt and pepper pattern, due to the existence of a great amount of multiplicative non-Gaussian noise, proportional to the intensity of the received signal [16].

In order to reduce this noise, known as *speckle*, multiple looks in the generation of the complex images can be employed, leading to degradation in spatial resolution. Another alternative to reduce speckle is through the use of filters, that can be either model-independent, such as Ordered Statistical Filters (OSF) [2], or model-dependent, such the Lee filter [10, 9], the Refined Lee filter [11] and SDNLM (Stochastic Distances and Nonlocal Means) [24], among others.

In [25] and [26], we introduced OWA filters, based on Ordered Weighted Average operators (OWA) [30], a family of mean operators that perform a convex combination of a set of ordered values, using a weight vector $\mathbf{w}$. In the same paper, we investigated the use of OWA filters to reduce speckle in SAR intensity imagery and proposed strategies to learn vector $\mathbf{w}$ using Genetic Algorithms (GA) [8] [6]. In [25], a single polarization (HH) was used with $3 \times 3$ windows, and in [26], 3 polarizations (HH, HV and VV) were used with $5 \times 5$ windows.

In the present work, we introduce WOWA filters, based on Weighted OWA operators (WOWA) [23]. This family of operators makes joint use of two vectors to weigh data: a vector $\mathbf{w}$, employed by OWA operators, and a vector $\mathbf{p}$, employed by Weighted Means operators. We focus on the use of WOWA filters in SAR imagery and compare the proposed approach with filters from the literature, using a series of experiments on synthetic images for a single polarization (HH), with $3 \times 3$ windows. Weight vectors

**p** and **w** are learned with GAs, having the Normalized Mean Square Error (NMSE) as fitness measure (see [1]).

This work is organized as follows. Sections 2, 3 and 4 discuss SAR images filters, WM, OWA and WOWA operators, and GAs, respectively. Sections 5 and 6 respectively describe WOWA filters and how to learn them using GAs. Section 7 presents an experiment in SAR imagery and Section 8 finally brings the conclusion.

## 2 Basic concepts on SAR imagery

Optical and SAR sensors measure the amount of energy reflected by a target in various bands of the electromagnetic spectrum, usually with frequencies found in the 2MHz to 12.5GHz range, and wavelengths ranging from 2.4cm to 1m. SAR systems generate the image of a target area by moving along a usually linear trajectory, and transmitting pulses in lateral looks towards the ground, in either horizontal or vertical polarizations [18], here respectively denoted as H and V.

Before the advent of polarimetric or polarized radars (PolSAR), the reception of the transmitted energy was made solely on the same polarization of the transmission, generating images in the HH and VV polarizations. With PolSAR, information about intensity and phase of the cross signals are also obtained, generating images in the HV and VH polarizations.

The imaging can be obtained by gathering all the intensity and phase information data from the electromagnetic signal after it has been backscattered by the target in a given polarization [12]. Each polarization in a given a scene generates a complex image, with the real and imaginary components for each pixel. We denote the complex images from HH, VV, and HV polarizations as $S_{\text{HH}}$, $S_{\text{HV}}$, and $S_{\text{VV}}$. Multiplying the vector $[S_{\text{HH}} \quad S_{\text{HV}} \quad S_{\text{VV}}]$ by its transposed conjugated vector $[S^*_{\text{HH}} \quad S^*_{\text{HV}} \quad S^*_{\text{VV}}]^t$, we obtain a $3 \times 3$ covariance matrix. The images in the main diagonal, denoted by $I_{\text{HH}}$, $I_{\text{HV}}$, and $I_{\text{VV}}$, contain intensity values.

### 2.1 Filters for SAR imagery

Given a window in an image, a filter substitutes the value of its central pixel by a function of the values of the pixels in the window. Two of the most weel-known filters are the mean and median filters, that employ the arithmetic mean and the median, respectively. In SAR imagery, the mean filter tends to reduce the speckle but it also tends to indiscriminately blur the image [13]. The median filter, on the other hand, reduces erratic variations by eliminating the lowest and highest pixel values [20].

The simplest filters are linear filters that employ the convolution operation. Given an image $I$, whose pixels take values in $R$, a $m \times m$ window around the central pixel $(x, y)$ in $I$, and a matrix of coefficients $\gamma : \{-m, ..., 0, ..., m\}^2 \to R$, the result of convolution for $(x, y)$ in the filtered image $I_\gamma$ is calculated as

$$I_\gamma(x, y) = \sum_{i=-m,m} \sum_{j=-m,m} \gamma(i, j) \times I(x + i, y + j).$$

Order Statistics Filters [2] constitute a general class of filters in which the result of filtering for a given pixel is the linear combination of the ordered values of the pixels

in the window around that pixel. They belong to the larger class of non-linear filters based on order statistics [17], being an application of L-estimators. An OSF is thus obtained when a convolution filter is applied on the ordered statistic of the pixel values in a window.

Other model-independent filters are the directional means filters, in which only pixels in one of the twelve regions of the six orthogonal directions are considered (diagonals, rows and columns) [20] and the local region filters (see [21]), in which the window is divided in eight regions based on angular position and the central pixel is replaced by the mean value of the subregion presenting the lowest variance.

More complex filters are obtained when a noise model is adopted. One of such filters is the so-called Lee filter, in which speckle reduction is based on multiplicative noise model using the minimum mean-square error (MMSE) criterion [10, 9]. The Refined Lee filter [11], here called R-Lee filter, is an improved version of the Lee filter, which uses a methodology for selecting neighboring pixels with similar scattering characteristics.

In [3], Buades et al. proposed the Nonlocal Means (NL-means) methodology, which consists in using similarities between patches as the weights of a mean filter, being well-suited for decreasing additive Gaussian noise. A more recent model-dependent approach, the SDNLM (Stochastic Distances and Nonlocal Means) filter [24], is an adaptive nonlinear extension of the NL-means algorithm filter. In this adaptive linear filter, overlapping samples are compared based on stochastic distances between distributions, and the $p$-values resulting from such comparisons are used to build the required weights.

### 2.2 Image Quality Assessment for SAR imagery

Assessing the performance of a filter, done by comparing the quality of the unfiltered and filtered images, is a very difficult task [28]. Two important indices to measure the quality of filtered images, NMSE and SSIM, are described bellow.

Index NMSE (Normalized Mean Square Error) is a general purpose error measure, widely used in image processing (see [1]). Let $r$ be the perfect information data and $s$ an approximation of $r$. NMSE is calculated as:

$$\mathrm{NMSE} = \frac{\sum_{j=1}^{n}(r_j - s_j)^2}{\sum_{j=1}^{n} r_j^2}, \tag{1}$$

where $r_j$ and $s_j$ refer to values in $r$ and $s$ at the same coordinates (the position of a given pixel in the case of images). NMSE always yield positive values, and the lower its value, the better is the approximation considered to be.

Index $\mathrm{SSIM}$ (Structural SIMilarity) measures the similarity between two scalar-valued images and can be viewed as a quality measure of one of them, when the other image is regarded as of perfect quality [29]. It is an improved version of the universal image quality index proposed proposed by [27]. This index takes into account three factors: (i) correlation between edges; (ii) brightness distortion; and (iii) distortion contrast. Let $r$ and $s$ be the perfect information and its approximation, respectively. $\mathrm{SSIM}$

is calculated as:

$$\mathrm{SSIM}(r,s) = \frac{\mathrm{Cov}(r,s)+\alpha_1}{\widehat{\sigma}_r\widehat{\sigma}_s+\alpha_1} \times \frac{2\overline{r}\,\overline{s}+\alpha_2}{\overline{r}^2+\overline{s}^2+\alpha_2} \times \frac{2\widehat{\sigma}_r\widehat{\sigma}_s+\alpha_3}{\widehat{\sigma}_r^2+\widehat{\sigma}_s^2+\alpha_3}, \tag{2}$$

where $\overline{r}$ and $\overline{s}$ are sample means, $\widehat{\sigma}_r^2$ and $\widehat{\sigma}_s^2$ are the sample variances, $\mathrm{Cov}(r,s)$ is the sample covariance between $r$ and $s$, and constants $\alpha_1, \alpha_2$ and $\alpha_3$ are used the index stabilization. SSIM ranges in the $[-1,1]$ interval, and the higher its value, the better is the approximation considered to be.

Other measures can be used to evaluate the quality of SAR imagery, such as, for instance, the equivalent number of looks (ENL), usually applied to intensity images in homogeneous areas, and index $\beta_\rho$, a correlation measure between the edges of two images (see [15]).

## 3 OWA and WOWA operators

The well-known Weighted Mean operators (WM) perform a convex combination of a set of values, using a weight vector **p**. In 1988, Yager [30] introduced the Ordered Weighted Average operators (OWA), in the Fuzzy Sets Theory domain. This family of mean operators perform a convex combination of a set of ordered values, using a weight vector **w**. In WM, the weights in **p** measure the importance of an information source with independence of the value that the source has captured, whereas in OWA, weights measure the importance of a value (in relation to other values) with independence of the information source that has captured it [23]. Weighted OWA operators (WOWA), proposed by Torra in 1997 [23], use both vectors **p** and **w** to weight data, and aims at taking advantage of both OWA and WM operators.

Let **p** be a weighting vector of dimension $n$ (**p** = $[p_1\ p_2\ ...\ p_n]$), such that:

- (i) $p_i \in [0,1]$;
- (ii) $\Sigma_i p_i = 1$.

A mapping $f_p^{wm} : R^n \to R$ is a Weighted Mean Operator (WM) of dimension $n$, associated to **p**, if:

$$f_p^{wm}(a_1,...,a_n) = \Sigma_i\ p_i \times a_i. \tag{3}$$

Let **w** be a weighting vector of dimension $n$ (**w**= $[w_1\ w_2\ ...\ w_n]$), such that:

- (i) $w_i \in [0,1]$;
- (ii) $\Sigma_i w_i = 1$.

A mapping $f_w^{owa} : R^n \to R$ is an Ordered Weighted Average operator (OWA) of dimension $n$, associated to a weighting vector **w**, if [30]:

$$f_w^{owa}(a_1,...,a_n) = \Sigma_i\ w_i \times a_{\sigma(i)}, \tag{4}$$

where $\{\sigma(1),...,\sigma(n)\}$ is a permutation of {1, ..., n} such that $a_{\sigma(i-1)} \geq a_{\sigma(i)}$, for all $i$ = {2,..., n} (i.e., $a_{\sigma(i)}$ is the $i$-th largest element in $\{a_1,...,a_n\}$).

The well-known mean, min, max and median operators are obtained straightforwardly with simple OWA $n$-ary vectors, denoted $\mathbf{w}_{mean}$, $\mathbf{w}_{min}$, $\mathbf{w}_{max}$, and $\mathbf{w}_{med}$, respectively. For example, for $n = 3$, we have: $\mathbf{w}_{mean} = [\frac{1}{3}\ \frac{1}{3}\ \frac{1}{3}]$, $\mathbf{w}_{min} = [0\ 0\ 1]$, $\mathbf{w}_{max} = [1\ 0\ 0]$, and $\mathbf{w}_{med} = [0\ 1\ 0]$.

Let **p** and **w** be weighting vectors as given above. A mapping $f_{w,p}^{wowa} : R^n \rightarrow R$ is a Weighted Ordered Weighted Average (WOWA) operator of dimension $n$, associated to **p** and **w**, if [23]:

$$f_{w,p,\phi}^{wowa}(a_1, ..., a_n) = \Sigma_i\ \omega_i \times a_{\sigma(i)}, \tag{5}$$

where $\{\sigma(1), ..., \sigma(n)\}$ is a permutation of {1, ..., n}, for all $i$ = {2,..., n}, such that $a_{\sigma(i-1)} \geq a_{\sigma(i)}$, weight $\omega_i$ is defined as

$$\omega_i = \phi(P_\sigma(i)) - \phi(P_\sigma(i-1)), \tag{6}$$

$$P_\sigma(i) = \Sigma_{j \leq i}\ p_{\sigma(j)}, \tag{7}$$

and $\phi$ is a monotone increasing function that interpolates points (0, 0) and $(\frac{i}{n}, \sum_{j \leq i} w_j)$, $i = 1, n$. Function $\phi$ is required to be a straight line when the points can be interpolated in a linear way. Torra [23] proves that the $\omega_i$'s compose a weighting vector of dimension n ($\omega = [\omega_1\ ...\ \omega_n]$), such that:

- (i) $\omega_i \in [0, 1]$;
- (ii) $\Sigma_i \omega_i = 1$.

In [23], we can also find examples of non-linear functions to implement $\phi$ and the proof that OWA and WM are particular cases of WOWA operators.

We now present a simple example to illustrate the use of WM, OWA, and WOWA operators. Let $a_1 = 10$, $a_2 = 20$, and $a_3 = 0$. We thus have $\sigma(1) = 2$, $\sigma(2) = 1$, and $\sigma(3) = 3$. Therefore $a_{\sigma(1)} = 20$, $a_{\sigma(2)} = 10$, and $a_{\sigma(3)} = 0$.

Let $\mathbf{w} = [.5\ .3\ .2]$ and $\mathbf{p} = [\frac{1}{6}\ \frac{2}{3}\ \frac{1}{6}]$. We thus obtain

- $f_w^{owa}(10, 20, 0) = .5 \times 20 + .3 \times 10 + .2 \times 0 = 13$,
- $f_p^{wm}(10, 20, 0) = \frac{1}{6} \times 10 + \frac{4}{6} \times 20 + \frac{1}{6} \times 0 = 15$.

Let $\phi_l$ be a linear by parts function, given by

$$\forall x \in (x_{k-1}, x_k], k \in \{1, n\}, \phi_l(x) = y_{k-1} + \frac{(x - x_{k-1})(y_k - y_{k-1})}{(x_k - x_{k-1})}, \tag{8}$$

where $\{(x_i, y_i)_{i=1,n}\}$ is a set of predetermined points. Using **w** to obtain the points $\{(x_i, y_i)_{i=1,n}\}$ as required in Equation 6 and applying them in Equation 8, we then have $\phi_l(0) = 0$, $\phi_l(\frac{1}{3}) = .5$, $\phi_l(\frac{2}{3}) = .8$ and $\phi_l(1) = 1$.

Using $\sigma$ and **p** above, we have $p_{\sigma(1)} = \frac{2}{3}$, $p_{\sigma(2)} = \frac{1}{6}$, and $p_{\sigma(3)} = \frac{1}{6}$. We then obtain $P_\sigma(1) = \frac{2}{3}$, $P_\sigma(2) = \frac{5}{6}$, and $P_\sigma(3) = 1$, as well as $\phi_l(P_\sigma(1)) = .8$, $\phi_l(P_\sigma(2)) = .9$, and $\phi_l(P_\sigma(3)) = 1$. Therefore $\omega_1 = .8$, $\omega_2 = .1$, and $\omega_3 = .1$. Thus

- $f_{w,p,\phi}^{wowa}(10, 20, 0) = .8 \times 20 + .1 \times 10 + .1 \times 0 = 17$.

## 4 Genetic algorithms

Genetic Algorithms (GA), first proposed in [8] (see also [6]), combine Mendel's ideas about the codification of life in genes, with Darwin's ideas on the survival of the fittest (natural selection). They are search algorithms that evolve populations of candidate solutions, according to a fitness function that assesses the quality of these solutions to solve the problem at hand.

A candidate solution $c \in C = \{c_1, \ldots, c_k\}$ consists of a set of parameters to a function $sol$, that models the problem at hand. Each $c$ can be thought of as a genotype (chromosome) and $sol(c)$ as its corresponding phenotype. A fitness function $fit$ evaluates the candidate solutions; $fit(sol(c))$ should be proportional to the capacity of $c \in C$ in solving the problem at hand.

At each GA iteration, three processes (selection, crossover and mutation) take place, generating a new population $C'$. The selection process is such that the fittest candidates in $C$ have a higher probability of being selected for reproduction. This process is usually performed by means of a roulette (the larger the fitness of an individual, the larger its share in the roulette wheel) or a set of tournaments (at each tournament, a set of individuals are chosen at random from the population and the winner is selected for reproduction). The reproduction process, called crossover, creates two new candidate solutions by mixing the genotypes of two selected parent candidate solutions. In the mutation process, all new candidate solutions can suffer changes, according to a (usually small) probability, called the mutation rate. Different forms of elitism can be used, by forcing the best candidates to be remain in the new population and/or to have a stronger influence on the creation of $C'$.

The first initial population is usually obtained randomly, but in many applications, the use of a selected set of chromosomes may lead to better results. The stop criterion is usually a fixed number of iterations. The combination of selection, crossover and mutation provide GAs with a good equilibrium between exploration and exploitation of the search space.

## 5 WOWA filters

In [25] and [26], we introduced a general class of filters, called OWA filters, that consist in applying OWA weight vectors (see [30]) in the values inside a sliding window over a given image. In the present paper, we propose the use of WOWA filters $F^{wowa}_{w,p,\phi}$, as described in the procedure below, to obtain a filtered image $I^{wowa}_{w,p,\phi}$ from a given image $I$, using WOWA operators (see [23]).

**Procedure** $F^{wowa}_{w,p,\phi}(I)$

1. Transform a weight matrix **M** associated to a predefined neighbourhood, into a vector with $n$ positions **p**.
2. For each pixel in position $(x, y)$ in the original image $I$, transform a window $I'$ around $(x, y)$, according to the predefined neighbourhood, into a vector of $n$ positions **a**.
3. Using **a**, derive $\sigma$ and $\mathbf{a}_\sigma$.
4. Using $\mathbf{w}_0$, $\mathbf{p}_0$ and $\phi_0$, derive weight vector $\omega$.
5. Calculate $f^{wowa}_{w,p,\phi}(a_1, ..., a_n)$.
6. Make the result become the value for position $(x, y)$ in the filtered image: $I^{wowa}_{w,p,\phi}(x, y) = f^{wowa}_{w,p,\phi}(a_1, ..., a_n)$.

Given an image $I$ and a position $(x, y)$ in $I$, and considering a $3 \times 3$ window, in step 2 we obtain vector **a**, with 9 positions, as $(I(x-1, y-1), I(x-1, y), I(x-1, y+1), I(x, y-1), I(x, y), I(x, y+1), I(x+1, y-1), I(x+1, y), I(x+1, y+1))$. Vector **p** is obtained in a similar way from **M** in step 1.

OWA and WM filters $F^{owa}_w$ and $F^{wm}_p$ are obtained in a similar but simpler way. Note that $F^{wm}_p$ is a convolution filter, whereas $F^{owa}_w$ is an OSF. A WOWA filter is a combination of convolution filters and OSFs, enjoying the advantages of both.

## 6 Learning WOWA filters with GAs

WOWA filters parameters can be can be either given or learned. In the following we study how to learn weight vectors associated to WOWA operators for SAR imagery using Genetic Algorithms (see Section 4).

### 6.1 Strategies for learning WOWA filters

We list below 3 ways to learn a filter $F^{wowa}_{w,p,\phi}$ for a given given image $I$, generating a filtered image $I^{wowa}_{w,p,\phi}$.

- WOWA-GA-wp: Learn vector **w** for filter $F^{owa}_w$, then learn vector **p**, by fixing **w**.
- WOWA-GA-pw: Learn vector **p** for filter $F^{wm}_p$, then learn vector **w**, by fixing **p**.
- WOWA-GA-p+w: Learn vectors **w** and **p** at the same time.

Considering a $m \times m$ window, the first two strategies consist of two consecutive learning processes in which each chromosome has $n = m^2$ positions. In the last strategy, each chromosome has $n = 2m^2$ positions.

### 6.2 GA details

Given an image, our experiments have been performed as follows. (a) the parameters of the distributions associated to the various regions in the image are estimated, (b) a set of simulated images is randomly created using the distributions parameters, (c) the set of simulated images is partitioned in two sets, one for training and one for testing, and

(d) the best weight vector found by the GA on the training set is used on the test set for evaluation.

As fitness function, we take the mean values of a given image index over the set of simulated images (see Section 2.2). Selection is done by usual methods, such as roulette or tournament (see Section 4). However, since the weight vectors sum up to 1, mutation and crossover are not straightforward.

Here crossover is made using a linear combination of the parent chromosomes weight values. Each chromosome has $n$ positions, each of which containing a real number (a weight), that sum up to 1 altogether. Given two parents $c_1$ and $c_2$, and random number $\alpha \in [0, 1]$, we generate two sons $c_{12}$ and $c_{21}$, where $\forall i \in \{1, ..., n\}$, $c_{12}[i] = \alpha \times c_1[i] + (1 - \alpha) \times c_2[i]$ and $c_{21}[i] = (1 - \alpha) \times c_1[i] + \alpha \times c_2[i]$. The values in $c_{12}$ and $c_{21}$ are then normalized to guarantee that the weights sum up to 1.

We tested a few strategies for mutation, and in the following we only relate the experiments on the ones that gave the best results, called A and B. In the experiments reported here, the mutation rate is not applied for each position but for the chromosome as a whole. If a chromosome is selected for mutation, then we randomly select a position $1 \leq q \leq n$ in the chromosome to be changed, considering a uniform distribution. Then the adopted strategies differ as follows:

- Strategy A: the value in position $q$ is multiplied by the mutation rate. The difference is divided by $n - 1$ and added to each of the remaining positions.
- Strategy B: the value in $q$ is increased with the value of its neighbour to the right (considering the chromosome as a ring), and the neighbour receives value 0.

## 7 Experiments

We conducted a series of experiments using a fragment of a phantom described in [19] (see Figure 3). In this study, we used only the L-band with wavelengths of [30cm, 1m] and frequencies of [1MHz, 2GHz].

To learn the weight vectors, we used a set of 50 synthetic images, simulated using the parameters for Wishart distribution estimated in [22] for an area in the Brazilian Amazon region, considering intensity images derived from polarization HH. Each simulated image has 240 $\times$ 240 pixels and was generated with 1-look. We used a $3 \times 3$ window and the weight vectors **p** and **w** thus have 9 positions each.

After a series of small experiments with various alternatives, we decided to fully test the proposed procedure considering the following parametrizations:

- Population size: 18, 36 and 72 elements
- Number of generations: 10 and 30
- Mutation strategies: A and B
- Mutation rates: .2 and .8
- Seeds for random numbers: 2, 70 and 271
- Selection type: roulette

For each experiment, we performed a 5-fold cross-validation, using 40 images for training and 10 for testing in each fold. The elements in the initial population in each experiment were chosen at random. As fitness function for each fold in each parametrization,

we took the means of the quality of the resulting filtered images, according to index NMSE (see Section 2.2).

Our experiments have shown that, as expected, the larger the number of generations and the larger the size of the population, the better the results. We have also verified that the seeds did have a significant influence on the results. In what regards the mutation strategies (A and B), as well as the mutation rates (.2 and .8), the results were quite similar.

The WOWA operator found by the GA that issued the best mean NMSE, considering the five folds, was obtained using seed 271, a population of 72 individuals, 30 generations, mutation strategy B with mutation rate .2. Table 1 brings the results obtained with filters whose parameters have been learned with the GAs, as well as other filters, considering the same type of window and the same number of folds. In the Table 1, we also report the results for SDNLM and R-Lee filters, with the best parametrizations chosen after a few experiments, using $5 \times 5$ filtering window for both filters, with $3 \times 3$ patches, and significance level of $5\%$ for for SDNLM, and with $\mathrm{ENL} = 1$ for R-Lee.

**Table 1.** NMSE and SSIM mean and standard deviation for 5 folds

| | NMSE | | SSIM | |
|---|---|---|---|---|
| | mean | std | mean | std |
| Simulated (no filter) | 0.9969 | 1.87E-4 | 0.0685 | 8.52E-7 |
| SDNLM | 0.0796 | 8.82E-6 | 0.1662 | 4.86E-6 |
| R-Lee | 0.0790 | 2.06E-6 | 0.1557 | 6.47E-6 |
| OWA-GA | 0.1118 | 1.12E-1 | 0.1365 | 4.61E-6 |
| WM-GA | 0.1173 | 2.21E-5 | 0.1376 | 4.67E-6 |
| WOWA-GA-pw | 0.1179 | 1.50E-4 | 0.1355 | 4.62E-6 |
| WOWA-GA-wp | 0.1070 | 1.71E-4 | 0, 1374 | 4.55E-6 |
| WOWA-GA-w+p | 0.1070 | 2.69E-4 | 0.1454 | 4.20E-6 |
| Mean | 0.1151 | 3.97E-6 | 0.1373 | 4.66E-6 |
| Median | 0.1893 | 7.91E-6 | 0.1076 | 5.40E-6 |
| Minimum | 0.8074 | 5.26E-6 | 0.0073 | 2.45E-7 |
| Maximum | 4.9708 | 1.15E-2 | 0.0394 | 1.66E-6 |

We see in Table 1 that the best NMSE mean results are obtained with Lee and SDNLM filters, and the worst with the minimum and maximum[1]. Among the WOWA filters learned with the GAs, those issued with strategies WOWA-GA-wp and WOWA-GA-w+p presented the best performance. Although in Table 1 they coincide with mean 0.1070, the exact mean NMSE value for WOWA-GA-wp and WOWA-GA-w+p are 0.1070922 and 0.1070894, respectively. For SSIM, the higher the better, and we see that a different order of quality is obtained. However, The three first positions are still held by the model-dependent filters and WOWA-GA-w+p.

[1] The NMSE values presented in Table 1 are slightly different from those reported in [25] and [26], due to rounding-up issues in the implementation of NMSE in different computer languages.

Figure 1 brings an unfiltered image and the filtered images obtained from it using some of the methods considered here. We note that even though obtaining a lower NMSE, the image produced by OWA-GA in Figure 5 is visually superior to those obtained with both complex filters; SDNLM produces a blurred image and the Lee filter yields a pixelated image.

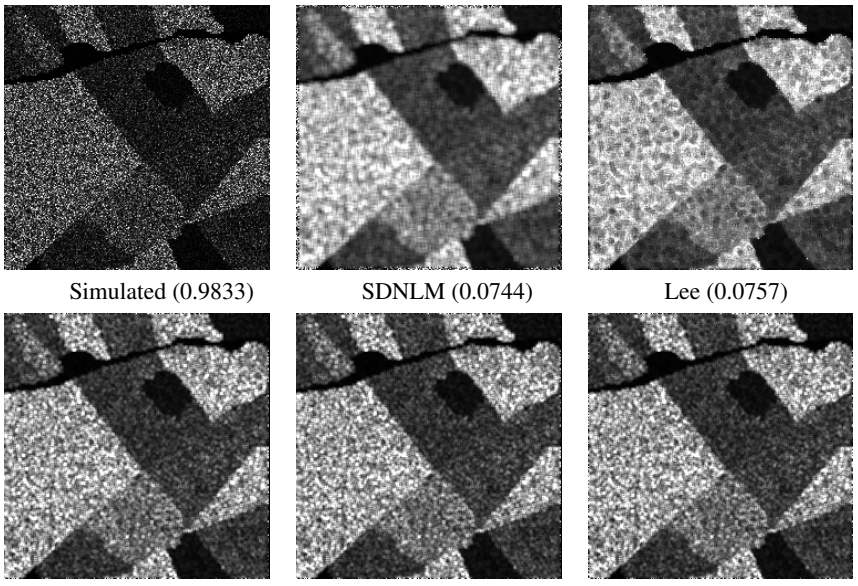


**Fig. 1.** Results considering the same HH simulated image, with NMSE inside parentheses

The GA was run on a machine with the following specifications: Intel i7, CPU 2.60 GHz, RAM with 16 GB, Windows 10, Fortran with Force 2.0 compiler. Considering 30 generations and 5 folds, with 10 images in each fold, and 72 elements in the population, the GA processing took approximately 1 hour, for no matter the value of the other parameters. As expected, the largest number of generations and the largest the populations, the longer the training process takes. Also, as the number of generations doubled, so roughly did the training time. Finally, as the size of the populations doubled, the training time was gradually lower than the double. The computational cost of using Wowa filters is reasonable in the context of the filtering radar images domain, and is close to the one obstines for Owa filters (see [25]).

The most important results here are:

– Learning **w** and **p** at the same time (WOWA-GA-p+w) outperformed the other alternatives, both in terms of quality and computational effort. Learning first **w** and then **p** (WOWA-GA-wp) led to similar quality results as WOWA-GA-p+w, but it took double the learning time.

– The learned weights for **p** in all experiments, considering a $3 \times 3$ window, could be partitioned in 3 values: one for the central pixel, one for the four pixels in the corners, and one for the four lateral pixels. This can be used advantageously to reduce the number of values to be learned by the GA.

## 8 Conclusions and future work

We have proposed a particular kind of filter based on order statistics, called WOWA filters. We have also studied how to learn the parameters for these filters (the WOWA weight vectors) to reduce speckle in SAR imagery using Genetic Algorithms. We have conducted some experiments on HH intensity images, with simulated images obtained from a real scene, using $3 \times 3$ windows. We compared the WOWA filter results with a set of filters, including OWA filters (a kind of Ordered Statistical Filters) and model-based filters SDNLM [24] and R-Lee [11]. WOWA filters with $3 \times 3$ windows outperformed OWA filters with $3 \times 3$ windows [25], but yielded worse results than other filters that used $5 \times 5$ windows (OWA, SDNLM and R-Lee filters) [26].

Our results point to directions for future research. We will now extend the work using $5 \times 5$ windows, the same size of windows used in the model-based filters considered here, with three polarizations. We expect this should lead to better results, based on past experiments: SDNLM and R-Lee filters with $5 \times 5$ windows outperformed OWA filters with $3 \times 3$ windows, but were outperformed by OWA filters with $5 \times 5$ windows.

The experiments performed here have shown us how to reduce the set of parametrizations to be tested when using larger windows, in order to compensate the expected increase in the learning process computational cost. These experiments have also shown us that instead of learning all the weights in vector **p**, we can use only a small set of values that are then conveniently replicated in the window.

In the future, we also intend to study the influence of initial populations in the GA, and address multi-optimization issues to learn the best weights considering more than one quality index.

## Acknowledgments

The authors are indebted to Vicenç Torra and to Lluis Godo for discussions on WOWA operators, and to Benicio Carvalho for providing computational resources.

## References

1. R. Baxter and M. Seibert. Synthetic aperture radar image coding. *MIT Lincoln Laboratory Journal*, 11(2):121–158, 1998.
2. A.C. Bovik, T.S. Huang, and D.C. Munson. A generalization of median filtering using linear combinations of order statistics. *IEEE Trans. on ASSP*, 31(6):1342—-1349, 2005.
3. A. Buades, B. Coll, and J. M. Morel. A review of image denoising algorithms, with a new one. *Multiscale Modeling & Simulation*, 4(2):490–530, 2005.
4. Christer Carlsson and Robert Fullér. *Fuzzy Reasoning in Decision Making and Optimization*. Studies in Fuzziness and Soft Computing Series. Springer-Verlag, 2002.

5. X. Fu, H. You, and K. Fu. A statistical approach to detect edges in SAR images based on square successive difference of averages. *IEEE GRSL*, 9(6):1094–1098, 2012.
6. D. E. Goldberg. *Genetic Algorithms in Search, Optimization, and Machine Learning*. Addison-Wesley, 1989.
7. F. Herrera. Genetic fuzzy systems: Status, critical considerations and future directions. *International Journal of Computational Intelligence Research*, 1(1):59–67, 2005.
8. J. H. Holland. *Adaptation in Natural and Artificial Systems*. Un. of Michigan Press, 1975.
9. J-S. Lee, M. R. Grunes, and G. de Grandi. Polarimetric SAR speckle filtering and its implication for classification. *IEEE Trans. on GRS*, 37(5):2363–2373, 1999.
10. J-S. Lee, M. R. Grunes, and S. A. Mango. Speckle reduction in multipolarization, multifrequency SAR imagery. *IEEE Trans. on GRS*, 29(4):535–544, 1991.
11. J.-S. Lee, M. R. Grunes, D. L. Schuler, E. Pottier, and L. Ferro-Famil. Scattering-model-based speckle filtering of polarimetric SAR data. *IEEE T. on GRS*, 44(1):176–187, 2006.
12. J.-S. Lee and E. Pottier. *Polarimetric Radar Imaging: From Basics to Applications*. Optical Science and Engineering. Taylor & Francis, 2009.
13. N. Mascarenhas. An overview of speckle noise filtering in sar images. In *1st Latin-American Seminar on Radar Remote Sensing - Image Processing Techniques*, pages 71–79, 1997.
14. A. Mittal, A. K. Moorthy, and A. C. Bovik. No-reference image quality assessment in the spatial domain. *IEEE Transactions on Image Processing*, 21(12):4695–4708, 2012.
15. E. Moschetti, M. G. Palacio, M. Picco, O. H. Bustos, and A. C. Frery. On the use of Lee's protocol for speckle-reducing techniques. *Latin American Applied Res.*, 36(2):115–121, 2006.
16. Harold Mott. *Remote Sensing with Polarimetric Radar*. John Wiley & Sons, 2006.
17. I. Pitas and A. N. Venetsanopoulos. *Nonlinear Digital Filters: Principles and Applications*. Springer, 2013.
18. J.A. Richards. *Remote Sensing with Imaging Radar*. Signals and Communication Technology Series, Springer, 2009.
19. M. F. S. Saldanha. *Um segmentador multinível para imagens SAR polarimétricas baseado na distribuição Wishart*. Phd Thesis, INPE, Brazil, 2013.
20. S.J.S. SantAnna and N. Mascarenhas. Comparação do desempenho de filtros redutores de "speckle". In *VIII SBSR*, pp 871–877, 1996.
21. Y. Sheng and Z.G. Xia. A comprehensive evaluation of filters for radar speckle suppression. In *IGARSS '96*, 3:1559 – 1561, 1996.
22. W. B. Silva, C. C. Freitas, S. J. S. Sant'Anna, and A. C. Frery. Classification of segments in PolSAR imagery by minimum stochastic distances between Wishart distributions. *IEEE J-STARS*, 6(3):1263–1273, 2013.
23. V. Torra. The weighted OWA operator. *Int. J. of Intelligent Systems*, 12(2):153–166, 1997.
24. L. Torres, S. J. S. Sant'Anna, C. C. Freitas, and A. C. Frery. Speckle reduction in polarimetric SAR imagery with stochastic distances and nonlocal means. *Pattern Recognition*, 47(1):141–157, 2014.
25. L. Torres, J. C. Becceneri, C. C. Freitas, S. J. S. Sant'Anna, S. Sandri, 2015. OWA filters for SAR imagery. In: *Proc. La-CCI'15, Curitiba, Brazil*, pp 1–6, 2015.
26. L. Torres, J. C. Becceneri, C. C. Freitas, S. J. S. Sant'Anna, S. Sandri. Learning OWA Filters parameters for SAR Imagery with multiple polarizations. In: *Bio-Inspired Computation & Applications in Image Processing*, (X.-S. Yang and J.P. Papa, eds), Elsevier, in print.
27. Z. Wang and A. C. Bovik. A universal image quality index. *IEEE SPL*, 9(3):81–84, 2002.
28. Z. Wang, A. C. Bovik, and L. Lu. Why is image quality assessment so difficult? In *IEEE ICASSP*, 4:3313–3316, Orlando, 2002.
29. Z. Wang, A. C. Bovik, H. R. Sheikh, and E. P. Simoncelli. Image quality assessment: From error visibility to structural similarity. *IEEE T. on Image Processing*, 13(4):600–612, 2004.
30. R.R. Yager. On ordered weighted averaging aggregation operators in multi-criteria decision making. *IEEE T. on Systems, Man and Cybernetics*, 18:183–190, 1988.